



Letter to the Editors

Elevated temperature fracture toughness of AISI 403 martensitic stainless steel

J.S. Dubey^{*}, S.L. Wadekar, J.K. Chakravartty*Materials Science Division, Bhabha Atomic Research Centre, Mumbai 400 085, India*

Received 24 November 1997; accepted 9 January 1998

Abstract

The AISI 403 martensitic stainless steel is used as the end fitting material in pressurised heavy water reactors. The fracture toughness of single quenched and tempered, double quenched and tempered, and Nb-modified variety of this steel has been evaluated at 473 and 573 K. Elevated temperature results are compared with the room temperature values reported in earlier studies. The double quenched and tempered and Nb-modified structures show higher toughness and dJ/da values at elevated temperatures. © 1998 Elsevier Science B.V.

1. Introduction

AISI 403 stainless steel in tempered martensitic condition is used as the end fitting material for pressurised heavy water reactors (PHWRs). It has excellent high temperature corrosion resistance, good elevated temperature mechanical properties and moderate irradiation resistance [1]. It also has a thermal coefficient of expansion value close to zirconium alloy pressure tube which is essential for producing leak tight mechanically rolled joints between end fittings and pressure tubes [2]. Ductile to brittle transition temperature (DBTT) of this steel in tempered martensitic condition is close to ambient and it has a low room temperature fracture toughness, K_{IC} , value of around 45 MPa m^{-1/2} [3]. End fittings operate at temperatures varying from 533 K to 588 K at pressure close to 10 MPa and they also undergo irradiation in service. The fracture toughness properties of this pressure boundary element is an essential part of the required data. Earlier studies have been made by authors to characterise and improve low

temperature fracture toughness of this high strength tempered martensitic steel by heat treatment and micro alloying [3,4]. It was found that homogeneous distribution of fine sized carbides precipitates of smaller aspect ratio gave significant improvement in room temperature fracture toughness and impact toughness values of tempered martensitic steels [3–7]. Double quenching and tempering heat treatment which results in refined grain structure and preferred carbide morphology was found to produce enhanced toughness in material along with lower DBTT [3–5]. Fracture toughness values of this material at end fitting operating temperatures have not been reported. This paper has the details of the results of J -integral fracture toughness tests carried out at elevated temperatures (473 K and 573 K) on unmodified and modified AISI 403 martensitic stainless steel.

2. Experiment

Two variants of AISI 403 steel, namely the conventional and the niobium modified varieties, used in this study were received in the form of solid forged blocks. The chemical composition of these blocks are given in Table 1. Few of the blocks of conventional AISI 403 were

^{*} Corresponding author. Tel.: +91-22 556 3060 extension 2210; fax: +91-22 556 0750, +91-22 556 0534; e-mail: mechmet@magnum.barct1.emet.in.

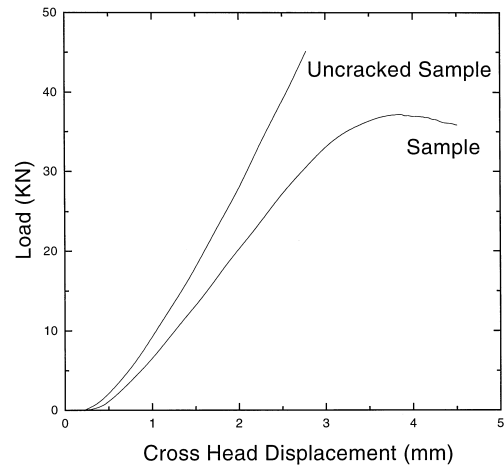
Table 1

Chemical composition of material under study (wt%)

	C	Cr	Mn	Si	S and P	Nb
AISI 403 (conventional)	0.11	12	0.25	0.16	< 0.02	–
AISI 403 (Nb modified)	0.11	12	0.2	0.18	< 0.02	0.1–0.2

further heat treated as shown in Table 2 making them double quenched and tempered structure. The heat treatment given and sample designation are as given in Table 2. Round tensile samples and 12.5 and 25 mm thick compact tension (CT) samples were machined from the heat treated blocks of the material. The microstructures in all the heat treated condition were observed using optical microscope, scanning electron microscope and transmission electron microscope. The details of which have been reported elsewhere [3,4].

Tensile tests were carried out in a screw driven test machine at a nominal strain rate of 10^{-4} at temperatures up to 573 K. The CT samples were fatigue precracked at room temperature as per ASTM E813-89 before fracture toughness testing. Elevated temperature J -integral tests were carried out in a screw driven test system without using any crack mouth opening displacement (COD) gage. The load line displacement were calculated from the cross head displacement values by deducting the extraneous displacement values which were found out by pulling an identical uncracked CT sample under same test conditions. The load–cross head displacement data during J -integral test on screw driven machine was logged in an interfaced computer. A sample load displacement plot for J -integral test is shown in the Fig. 1 along with the same plot for an uncracked sample at 473 K. A computer programme was developed to calculate the J -integral values, from digitally recorded load and cross head displacement values, after correcting cross head displacement values for the slack in load train, initial non-linear displacements and elastic deflection of the uncracked sample. The compliance, during the linear loading portion of the calculated load–load line displacement plot, gave an estimate of crack length which was within 4% of the actual physical crack length measured after the test. The samples were fatigue cracked after J -integral test to delineate the crack growth (Δa) during the test. The fatigue precracked length and Δa values were

Fig. 1. Tensile pull plot in J -test at 473 K.

physically measured by nine point averaging method specified by ASTM E813-89.

3. Results

The tensile properties of all the three material tested are given in Table 3. The yield strength, ultimate tensile strength and break strain values are plotted as a function of temperature in Fig. 2. The tensile test data was analysed to get the work hardening behaviour of the materials. The calculated Holloman work hardening coefficient (n) and Ramberg–Osgood fit parameters, as per Eqs. (1) and (2) respectively, are also given in Table 3.

$$\sigma = K \varepsilon_p^n, \quad (1)$$

$$\varepsilon/\varepsilon_0 = (\sigma/\sigma_0) + \alpha(\sigma/\sigma_0)^n, \quad (2)$$

where ε and σ are the true strain and stress, ε_p is the true plastic strain. σ_0 has been taken as 0.2% yield strength and $\varepsilon_0 = \sigma_0/E$ where E is the young's modulus which was taken to be 190 GPa.

Decrease in yield and ultimate tensile strength and little change in break strain values were seen with increasing temperature for all the three structures. The work hardening behaviour of these materials also remained nearly

Table 2

Heat treatment and designation of the material

Material	Heat treatment	Designation
AISI 403 (conventional)	Austenitise at 910°C, 40 min soak, oil quench, temper at 610°C—4 h	QT
AISI 403 (conventional)	Austenitise at 1040°C, 30 min soak, oil quench, reheat to 850°C, 30 min soak, oil quench, temper at 610°C for 4 h	DQT
AISI 403 (Nb modified)	Austenitise at 950°C—45 min soak, oil quench, temper at 670°C for 4 h	NQT

Table 3
Tensile properties of materials tested

Material	Temperature (K)	Yield strength (MPa)	Ultimate tensile strength (MPa)	Uniform strain (mm/mm)	Break strain (mm/mm)	<i>n</i>	Ramberg–Osgood fit parameters	
							α	<i>n</i>
AS	297	525	710	0.09	0.18	0.13	1.65	7.4
	473	535	665	0.05	0.14	0.1	1.28	9.5
	573	434	597	0.07	0.15	0.12	1.34	7.9
NQT	297	675	803	0.04	0.13	0.09	0.85	11.5
	473	609	711	0.03	0.09	0.07	0.6	13.5
	573	593	695	0.03	0.12	0.08	0.84	12.6
DQT	297	580	727	0.07	0.26	0.11	1.6	8.8
	473	556	632	0.08	0.28	0.12	1.16	8.4
	573	480	578	0.05	0.22	0.08	1.18	11.5

Table 4
Fracture toughness test results

Temperature (K)	AS		NQT		DQT	
	J_{IC} (kJ m ⁻²)	d <i>J</i> /d <i>a</i> (MPa)	J_{IC} (kJ m ⁻²)	d <i>J</i> /d <i>a</i> (MPa)	J_{IC} (kJ m ⁻²)	d <i>J</i> /d <i>a</i> (MPa)
297 ^a	100	—	—	—	160	183
473	101	119	128	184	176	197
573	135	22	111	162	117	165

^aFrom Ref. [3].

unchanged as indicated by the Ramberg–Osgood work hardening fit constants. Fig. 3 gives the *J*-integral (*J*) vs. crack extension (Δa) plots obtained at 473 K. The plot shows large scatter in *J* values for AS structure with a J_{IC}

value of around 100 kJ m⁻² and a lower bound d*J*/d*a* value of 110 MPa. It can be seen that at 473 K DQT structure has the highest crack initiation and crack propagation toughness, which are listed in Table 4. Fig. 4 compares the *J*– Δa values obtained at 573 K for all the structures. At 573 K, the DQT and NQT structures showed

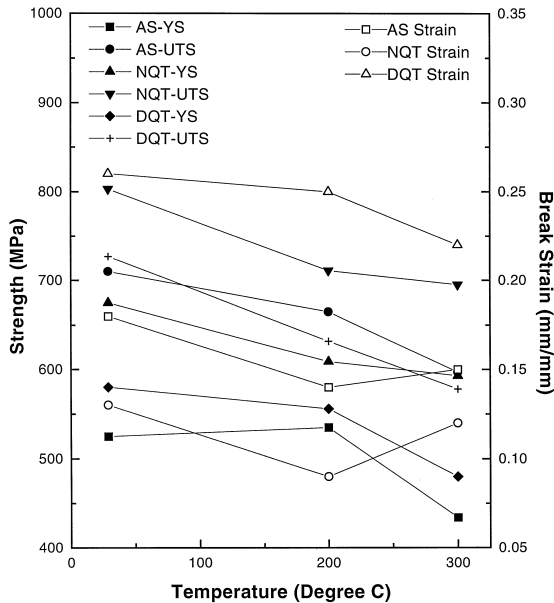


Fig. 2. Tensile properties as a function of temperature.

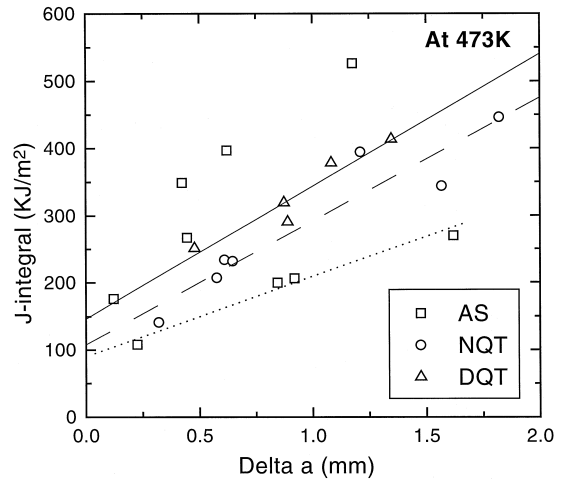


Fig. 3. *J*– Δa plot at 473 K.

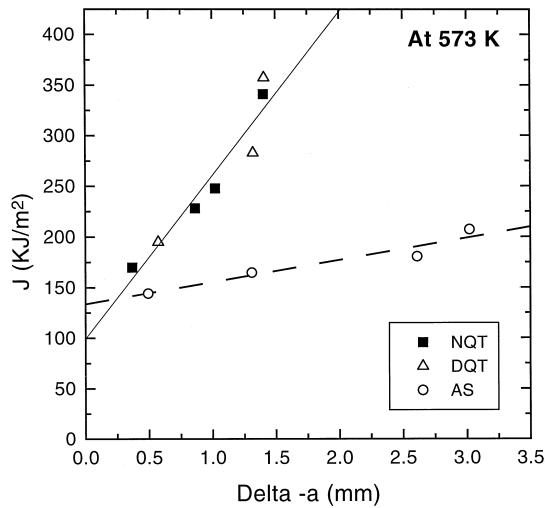


Fig. 4. $J-\Delta a$ plot at 573 K.

nearly identical fracture toughness near the onset of stable crack growth and comparable dJ/da value.

As can be seen from the data of Table 4 elevated temperature J_{IC} values do not change much from that of at ambient temperature. The large scatter in J -integral values of AS structure continues to be present at 473 K. A reduction in dJ/da values seen at 573 K should be verified by carrying out additional tests to confirm that this lower value is not due to the statistical scatter alone. As there is little difference in tensile properties, work hardening behaviour and toughness levels it seems likely that fracture mode remains same from ambient temperature to 573 K. The improvement in toughness levels of DQT and NQT structures has been attributed to the finer grain structure and lower aspect ratio of carbides which are more

homogeneously distributed in these structures [3,4]. It appears that these factors continue to give better toughness at 573 K to the DQT and NQT structures.

4. Summary and conclusion

Above elevated temperature tests showed that work hardening behaviour and fracture initiation toughness of AS, DQT and NQT materials do not change appreciably from that at ambient temperature. In AS structure, large scatter in J -integral values was observed even at elevated temperatures. The DQT and NQT material show much higher initiation toughness and $J-\Delta a$ curve slope at all the testing temperatures employed in this study. These structures also showed reduced scatter in J -integral values.

References

- [1] C.K. Gupta, Materials in Nuclear Energy Applications, Vol. 1, CRC Boca Raton, FL, 1989.
- [2] R.R. Hobsons, J.K. Macpherson, in: Materials in Nuclear Energy, Ohio, 1982, pp. 37–43.
- [3] C. Gupta, J.S. Dubey, S. Ganguly, A.R. Biswas, Y.V. Kamat, J.K. Chakravarty, High Temp. Mater. Proc. 16 (1) (1997) 65–75.
- [4] C. Gupta, S.L. Wadekar, J.S. Dubey, R.T. Savalia, K.S. Balakrishnan, S. Anantharaman, Y.V. Kamat, J.K. Chakravarty, High Temp. Mater. Proc. 16 (2) (1997) 149–157.
- [5] E. Chang, C.Y. Chang, C.D. Liu, Metall. Trans. 25A (1994) 545–555.
- [6] M. Sarikaya, B.G. Steinberg, G. Thomas, Metall. Trans. 13A (1982) 2227–2237.
- [7] B.V. Narasimha Rao, G. Thomas, Metall. Trans. 8A (1977) 1439–1448.